Simulation of unidirectional solidification with a tilted crystalline axis

Tomohiro Okada and Yukio Saito
Department of Physics, Keio University, 3-14-1 Hiyoshi, Kohoku-ku, Yokohama 223, Japan
(Received 15 February 1996)

Tilting of the crystal profile during directional solidification is studied numerically, when the crystalline axis is misoriented from the temperature gradient and the pulling direction. Only with the anisotropy in surface stiffness is the crystal shown to tilt to an angle ϕ smaller than the misorientation of the crystalline axis ψ. The angle ϕ approaches ψ on increasing the pulling velocity V, as is often observed in experiments. The V dependence of the tilting ϕ thus does not necessarily mean that the tilting is caused by the kinetic effect. With $\psi=45°$ we observe tip splitting and double fingers, a constituent of the compact seaweed pattern. [S1063-651X(96)05907-7]

PACS number(s): 81.10.Aj, 47.20.Hw, 82.40.Ck

I. INTRODUCTION

Pattern formation is an intensively studied subject in nonlinear and nonequilibrium statistical physics. Dendritic growth is its typical example, and the anisotropy in the surface free energy is shown to play an essential role in stabilizing the dendrite tip when the dendrite is growing in the free space [1–4].

In contrast to the free dendrite, directional solidification is performed under a temperature gradient. The average interface lies normal to the gradient, but with a fast pulling rate the interface undergoes various modulations as periodic arrays of cells, cusps, and dendrites. Usually, the crystalline axis is set parallel to the direction of the temperature gradient and the pulling direction. The realized cellular patterns have symmetry around the crystal axis. If the crystalline axis is oriented differently from the temperature gradient, a tilted cellular structure is observed in experiments [5–8]. In the linear stability analysis, the anisotropy in the surface free energy is shown to be irrelevant to the tilting and the anisotropic kinetics is responsible for producing the effect [9,10]. But since the neutral curve is very flat near the critical velocity V_c, various modes couple nonlinearly even near V_c. The anisotropy of the surface free energy may be relevant for the fully nonlinear regime.

One of the authors has previously simulated the interface deformation in the directional solidification numerically when the orientation of the crystalline axis coincides with that of the temperature gradient [11]. The interface takes a periodic array of cellular structure near the supercritical bifurcation point. The tip of the cellular interface is quite rounded and the whole profile is far from parabolic. The interface becomes dendritic with a pointed tip only far from the bifurcation point. This indicates that the free-energy anisotropy governs the interface shape for fast growth, whereas the temperature gradient controls and stabilizes the cellular structure for low growth rate or near the stability limit of the planar interface. If the orientation of the interface tension is different from that of the temperature gradient, the two tip-stabilizing mechanisms may compete and lead to the tilting of the periodic structure. This phenomenon is actually observed by Akamatsu *et al.* by solving the time-dependent diffusion equation on multiple lattices [7]. Here we study the problem systematically by means of a boundary element method [12] in a quasistationary approximation that is an extension of the method used previously [11]. The method cannot describe the full dynamics, but it is valid in the steady state. The method is also free from the lattice anisotropy that can be induced by the lattice grids to solve the diffusion equation. We study the variation of the tilt angle ϕ of the crystal on increasing the angle ψ between the crystallographic orientation and the direction of the temperature gradient.

II. MODEL AND SIMULATION METHOD

In the experiment of the directional solidification, the solution is contained in a thin cell, called a Hele-Shaw cell, and placed in a temperature gradient. The direction of the temperature gradient is taken as the z axis. The cell is pulled in the negative-z direction to the colder region with the velocity V and thus the crystal grows with the same growth velocity V.

The concentration of the solution is denoted by c_∞. Due to the material conservation, the average concentration in the solid should be c_∞ in the steady growth situation. When the interface deforms from the planar structure, the local concentration $c_S(\mathbf{r})$ on the solid side of the interface is different from, but close to, c_∞. For an atomically rough interface above the roughening temperature, the surface kinetics is fast. With the approximation of an infinitely fast kinetics, the local equilibrium at the interface is guaranteed. Then the concentration at the liquid side of the interface c_L should be as high as c_S/k with the equilibrium segregation coefficient k. The concentration difference in the liquid near and far from the interface induces the diffusion flow $\mathbf{J}=-D_c\nabla c$, which transports the excess material expelled by the solidification:

$$v_n(c_L-c_S)=-D_c\frac{\partial c}{\partial n}. \tag{1}$$

Here v_n is the normal growth rate and D_c is a chemical diffusion constant.

When the solid is in equilibrium with the liquid with concentration c_L, the interface temperature T_S should be lower than the melting temperature of the pure system T_M as

$$T_S = T_M(1-\tilde{\gamma}\kappa) - mc_L, \tag{2}$$

with the surface stiffness $\tilde{\gamma}$, the curvature κ, and the slope of the liquid line m.

Due to the fast thermal diffusion, the temperature gradient $G_T = dT/dz$ is well approximated to be constant and the temperature profile is linear as

$$T(z) = T_M - \frac{mc_\infty}{k} + G_T z. \tag{3}$$

The origin of the z axis is so chosen to lie at the position of the planar interface. The concentration c_L at the interface $z=\zeta(x)$ is thus determined from Eqs. (2) and (3) as

$$c_L = \frac{c_\infty}{k} - \frac{T_M\tilde{\gamma}}{m}\kappa - \frac{G_T}{m}\zeta. \tag{4}$$

We normalize the field by the miscibility gap $\Delta c = c_\infty(1/k-1)$ in the dimensionless form u as

$$u(x,z,t) = \frac{c-c_\infty}{\Delta c}. \tag{5}$$

The far field condition is $u(z\to\infty)=0$. The diffusion equations with boundary conditions at the interface are now written as

$$\frac{\partial u}{\partial t} = D_c\nabla^2 u, \tag{6a}$$

$$u_S = 1 - d\kappa - \frac{\zeta}{l_T}, \tag{6b}$$

$$[k+(1-k)u_S]v_n = -D_c\frac{\partial u}{\partial n}. \tag{6c}$$

Here $d = T_M\tilde{\gamma}/m\Delta c$ is the capillary length and $l_T = m\Delta c/G_T$ is the thermal length.

When the stiffness $\tilde{\gamma}$ is the smallest in the z direction, the array is symmetric around the z axis. But when the crystalline axis is off from the pulling direction, the crystal profile may tilt. Assume that the stiffness $\tilde{\gamma}$ is minimum in the orientation with the angle ψ from the z axis, then the capillary length takes the form

$$d = d_0[1-\alpha\cos 4(\theta-\psi)] \tag{7}$$

for an interface with its normal vector making an angle θ to the z axis. Here we assume fourfold symmetry in the surface tension. As a result, the crystal tilts with an angle ϕ and the interface deformation drifts transversally with the velocity $v_x = V\tan\phi$. In the frame moving with the same velocity $\mathbf{v}=(v_x,V)$ with the growth front, the diffusion equation is written as

$$\hat{L}u = \frac{2}{l_D}\tan\phi\frac{\partial u}{\partial x} + \frac{2}{l_D}\frac{\partial u}{\partial z} + \nabla^2 u = \frac{1}{D_c}\frac{\partial u}{\partial t} = 0. \tag{8}$$

Here $l_D = 2D_c/V$ is the diffusion length. In the last equality we use the quasistationary approximation such that the diffusion field relaxes quickly compared to the interface deformation.

The angle ϕ of the crystal profile may differ from the angle ψ of the crystalline axis. When the thermal gradient provides the anisotropy necessary for the tip stability of the cellular structure, the angle ϕ would be small. When, on the other hand, the surface free energy dominates, the angle ϕ would be close to ψ. We study the variation of the angle ϕ as a function of the pulling rate V.

Numerical simulation follows the previous boundary element procedure [11,12]. The diffusion equation is transformed in the integro-differential equation of the interface Γ by means of the Green's theorem as

$$\int d\Gamma' g(\mathbf{r},\mathbf{r}')\frac{\partial u(\mathbf{r}')}{\partial n} = \int d\Gamma' h(\mathbf{r},\mathbf{r}')u_S(\mathbf{r}'). \tag{9}$$

Here g is the Green's function of the operator $\hat{L}^\dagger$ adjoint to $\hat{L}$, defined in Eq. (8) as

$$\hat{L}^\dagger g = \nabla^2 g - \frac{2}{l_D}\tan\phi\frac{\partial g}{\partial x} - \frac{2}{l_D}\frac{\partial g}{\partial z} = -\delta(\mathbf{r}-\mathbf{r}'). \tag{10}$$

It is explicitly written as

$$g(\mathbf{r},\mathbf{r}') = \frac{1}{2\pi}\exp\left[-\frac{1}{l_D}(\Delta z + \Delta x\tan\phi)\right]K_0\left(\frac{\rho}{l_D\cos\phi}\right), \tag{11}$$

with $\Delta z = z-z'$, $\Delta x = x-x'$, $\rho = \sqrt{(\Delta x)^2+(\Delta z)^2}$, and K_0 being the modified Bessel function of zeroth order. The integral kernel h is given as

$$h(\mathbf{r},\mathbf{r}') = \frac{\partial g}{\partial n'} - \frac{2}{l_D}[n_z' + n_x'\tan\phi]g(\mathbf{r}-\mathbf{r}') - \frac{1}{2}\delta(\mathbf{r}-\mathbf{r}'). \tag{12}$$

When the interface becomes periodic with periodicity λ, it is sufficient to consider one period. By discretizing this one period with N grid points, the integral equation (9) is transformed into the matrix form as

$$\sum_{m=-\infty}^{\infty}\sum_{j=1}^{N} G_{ij+mN}q_j = \sum_{m=-\infty}^{\infty}\sum_{j=1}^{N} H_{ij+mN}u_j, \tag{13}$$

where m denotes the periodic images of the interface in consideration. Here u_j and q_j are the values of diffusion field and its normal gradient at the interface on the jth grid point and the matrix G and H are obtained by the integration of g and h on a segment. The detailed procedure is described in previous works [11,13].

For a given profile $z=\zeta(x,t)$ under the given pulling rate V and the tilt angle ϕ, we can calculate G and H and also the interface values of u_j from the local equilibrium condition Eq. (6b). Then the matrix equation (13) is solved to give the gradient $q=\partial u/\partial n$, which determines the local velocity of the interface from the conservation condition Eq. (6c). The interface is advanced accordingly to a new profile. For a directional solidification, the pulling rate V in the z direction

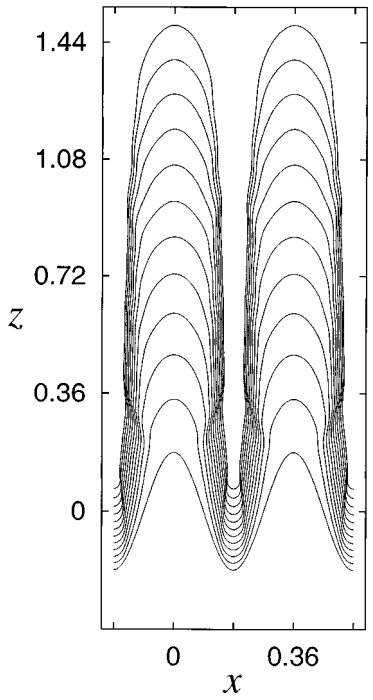

FIG. 1. Time evolution of a symmetric pattern of an interface with a crystalline axis oriented to the pulling direction z. The pulling velocity is $V/V_c=6.72$.

is controlled externally. The transversal velocity $v_x=V\tan\phi$, on the other hand, should be determined self-consistently.

We start the simulation by supposing that the frame has some transversal velocity $V\tan\phi$. After some time of simulation the interface tilts and the tip of the cellular pattern acquires some transversal velocity. The tip here means the interface position with the maximum curvature near the topmost part. Since the tip is fluctuating in every time step due to the discreteness of grids and the inaccuracy of numerical integration, we define the tilt angle of the tip $\phi_{\rm tip}$ in a coarse-grained sense. It is defined from the slope of two consecutive tip positions after a sufficiently long time interval dt:

$$\phi_{\rm tip}=\tan^{-1}\frac{y(t+dt)-y(t)}{x(t+dt)-x(t)}. \tag{14}$$

Then the angle ϕ of the moving frame is relaxed to $\phi_{\rm tip}$ as

$$\phi(t+dt)=\phi(t)-\frac{dt}{\tau}[\phi(t)-\phi_{\rm tip}], \tag{15}$$

with the appropriate relaxation time τ [14]. In the stationary state in which we are interested, tilt angle ϕ should remain constant and it agrees with $\phi_{\rm tip}$.

III. SIMULATION RESULTS

We have chosen the same parameter sets that have been used previously to simulate steel with impurities of Cr and Ni [11,13]. The equilibrium segregation coefficient is $k=0.9$. The length and time units are chosen such that the thermal length is unity $l_T=1$ and the chemical diffusivity is unity $D_c=1$. The capillary length is then $d_0=2.95\times10^{-4}$.

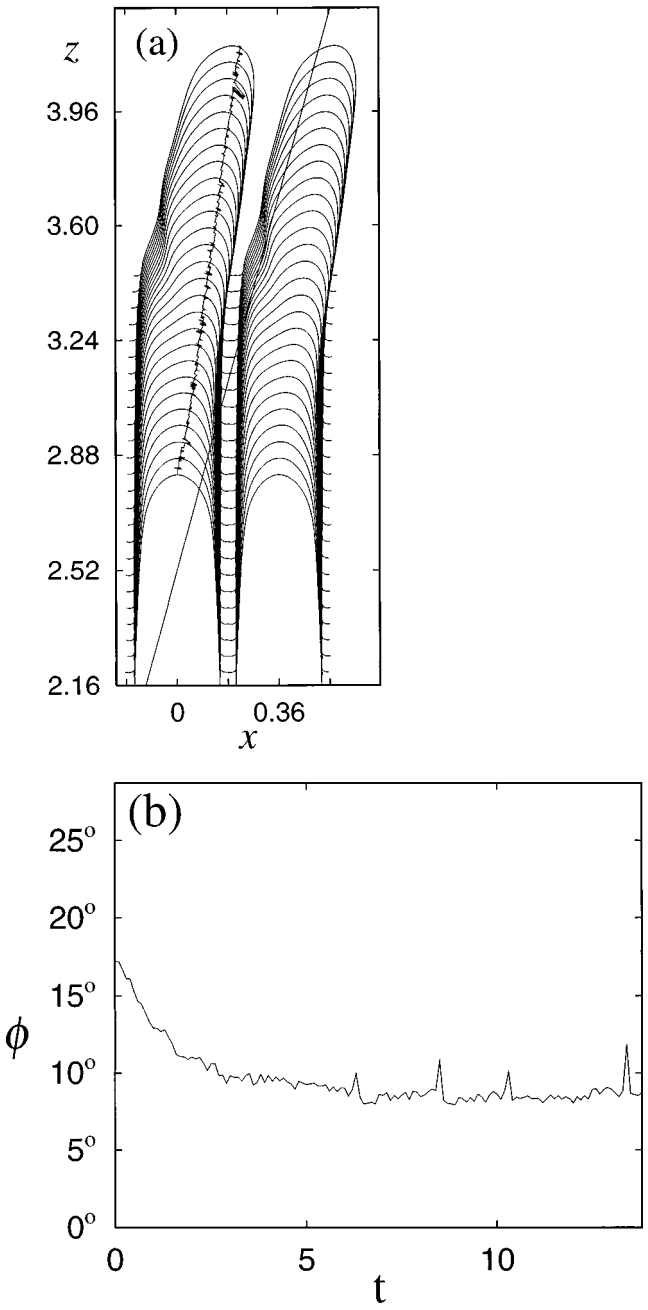

FIG. 2. (a) Initial transient of the time evolution of a tilted crystal with the line representing the tip trajectory. The crystalline axis is oriented $\psi=17°$ off from the z axis, whereas the profile tilts only $\phi=8.8°$. The pulling rate is $V/V_c=3.50$. (b) Temporal relaxation of the tilt angle ϕ of the frame that is related to the transversal velocity $v_x=V\tan\phi$ of the moving frame.

The anisotropy in the surface stiffness is assumed to be $\alpha=0.1$. The critical growth rate is calculated to be $V_c=1.14$, with the critical wavelength $\lambda_c=2\pi/q_c=0.5$. The simulated system is assumed to have periodicity $\lambda=0.36$, as was done previously [11]. In fact, in the previous simulation we assumed that the interface takes an array of symmetric fingers and mirror images are imposed at both boundaries to simulate only a half period to save CPU time. In the present simulation we want to realize tilted fingers and the whole period is necessary with periodic boundary conditions.

Starting from a sinusoidally modulated interface, we first

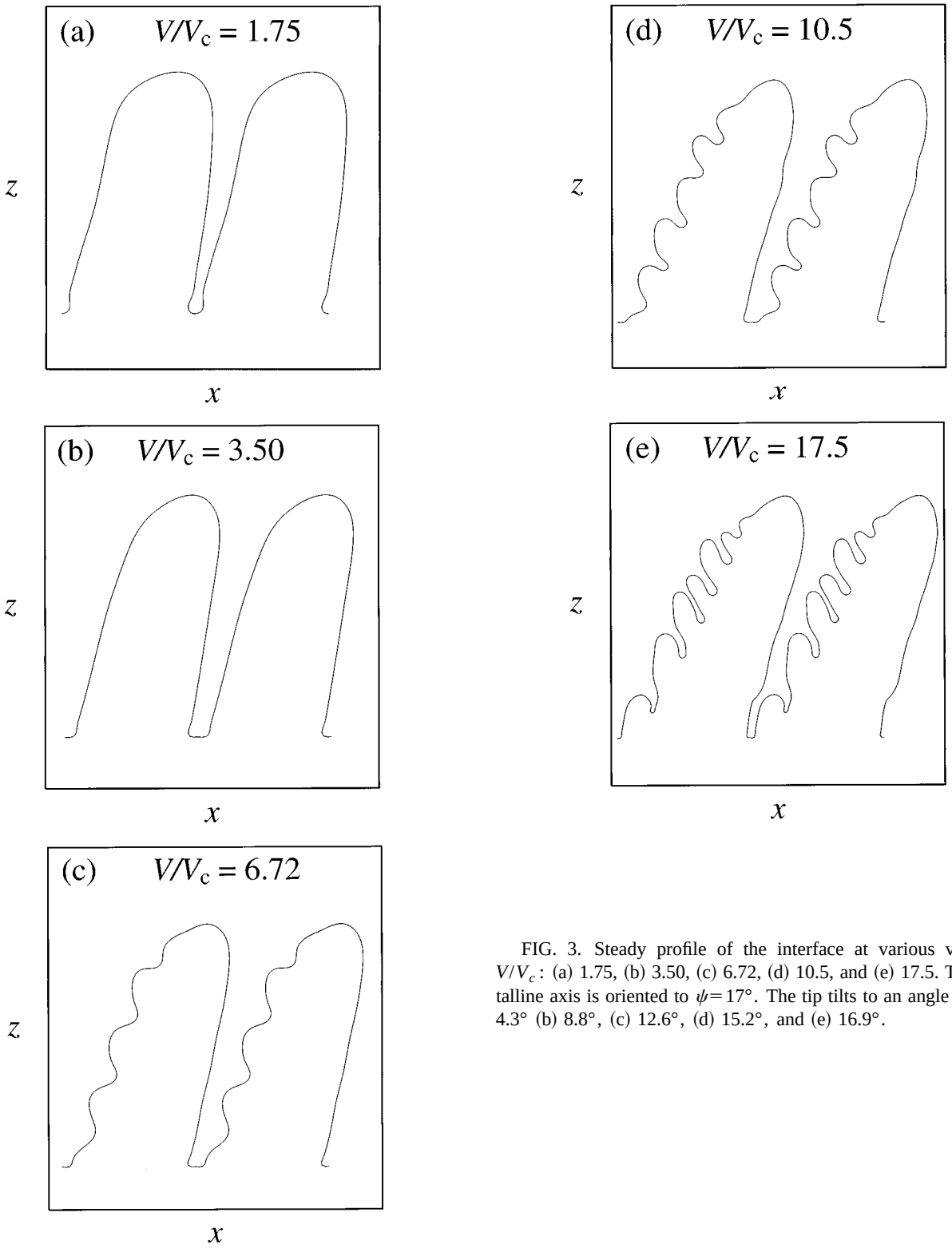

FIG. 3. Steady profile of the interface at various velocities V/V_c: (a) 1.75, (b) 3.50, (c) 6.72, (d) 10.5, and (e) 17.5. The crystalline axis is oriented to $\psi = 17°$. The tip tilts to an angle ϕ as (a) 4.3° (b) 8.8°, (c) 12.6°, (d) 15.2°, and (e) 16.9°.

simulate the symmetric finger with a crystalline axis lying parallel to the pulling direction $\psi = 0$. The profile of the previous simulations is reproduced even with the different boundary conditions. Figure 1 shows an example of the time development of cuspate fingers for $V/V_c = 6.72$. In the following figures we show two periods of the profile. The maximum grid spacing along the interface is chosen to be $d_{\max} = 0.03$, small enough compared to the tip radius $\rho = 0.12$. From the final configuration of this finger, we start the simulation of the tilted finger.

A. Tilt angle at various pulling rates

The orientation ψ of the crystalline axis with the minimum surface stiffness is fixed to a constant value $\psi = 0.30$ rad $= 17°$. We vary the pulling rate V and observed the tilting of the interface profile. The initial transversal velocity $v_x = V\tan\phi$ of the moving frame is given by $\phi = \psi$, but

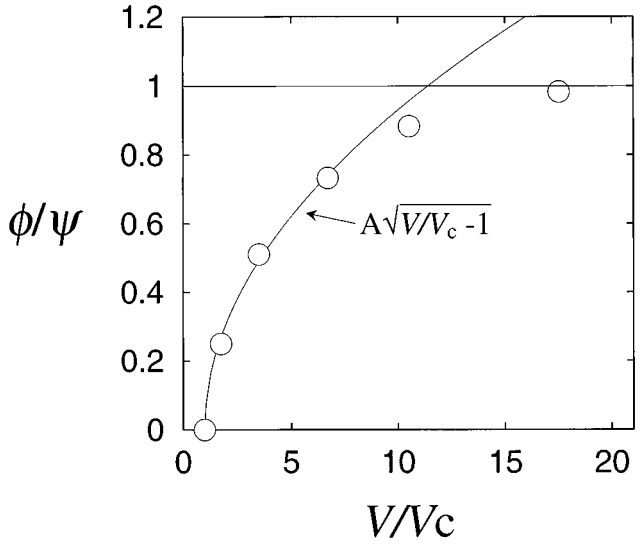

FIG. 4. Ratio of the tilt angle ϕ to the imposed crystalline tilting ψ at various pulling rates V/V_c. The crystalline axis is oriented to $\psi=17°$.

the angle ϕ is gradually relaxed to the tilt angle of the tip ϕ_{tip} by Eq. (15). By the insertion and rearrangement of mesh points, a numerical fluctuation is induced locally, but on average the system reaches the steady state asymptotically at all the pulling velocities studied, as shown in Fig. 2(b). At low velocities, the tilt angle ϕ of the crystal is smaller than the imposed angle ψ by the surface stiffness, as shown in the profile evolution in Fig. 2(a). The trajectory of the maximum curvature point is almost parallel to the inclination of the narrow groove. Therefore, the tilt angle of the crystal ϕ can be defined from the inclination of the groove in the steady-state profile of the interface. The steady profiles of the interface at different velocities are depicted in Fig. 3. On increasing the velocity, fingers tilt steeper with stronger asymmetries in the sidebranch structures: When the dendrite tilts to the right, branches on the left-hand side have a larger

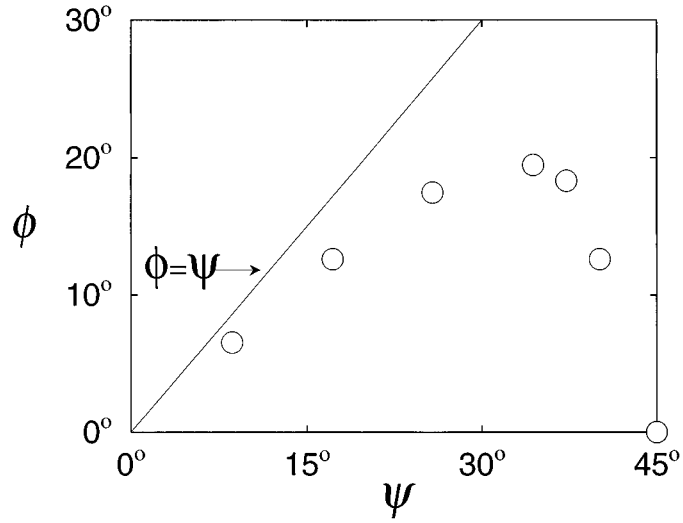

FIG. 5. Tilt angle ϕ at various crystalline orientations ψ. The pulling velocity is fixed to $V/V_c=6.72$.

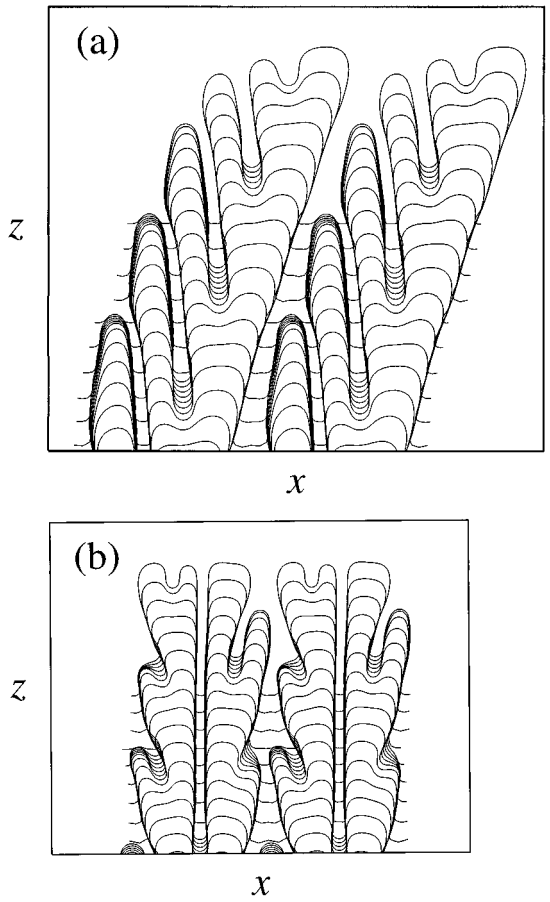

FIG. 6. Steady profile of the interface at various orientations of the crystalline axis: (a) $\psi=37°$ and (b) $\psi=45°$. The pulling velocity is fixed at $V/V_c=6.72$.

deformation than those on the right-hand side. The asymmetry results because the left-hand side of the tip faces the open space and the diffusion field in front is expected to vary much, whereas the right-hand side is shielded by the tip itself and the diffusion field varies little. The noise amplification should thus be larger on the left-hand side than on the right.

The tilt angle ϕ varies as a function of the pulling rate V, as shown in Fig. 4. Near V_c it increases almost parabolically to the velocity difference from the critical value $V-V_c$ and at a large pulling rate it reaches the orientation of the crystalline axis ψ. Usually, large tilting at the large pulling rate is interpreted as evidence of the kinetic mechanism for tilting. The present simulation shows that the surface free energy brings the same tendency that ϕ increases with V.

B. Tilt angle for various crystalline orientation

We now fix the pulling rate at $V/V_c=6.72$ and vary the tilting of the crystalline axis ψ. The tilt angle ϕ of the profile is shown in Fig. 5 as a function of ψ. At small ψ, ϕ is almost linearly proportional to ψ, but soon the angle ϕ becomes smaller than ψ because the transversal motion of the primary dendrite is suppressed by the neighboring dendrite. Increasing ψ further, the sidebranches of the next dendrite prevent the transversal shift of the primary dendrite, as shown in Fig. 6(a), and ϕ decreases. Near the angle $\psi=\pi/4$, the randomness of the sidebranch formation leads

the irregular meandering of the position of the maximum curvature and the tilt angle ϕ is not well defined. At $\psi=\pi/4=45°$, the interface normal to the z direction splits to the left and right fingers, but both interfere strongly in our small system and their tips split again irregularly, as shown in Fig. 6(b). Thus the system consists of an irregular arrangement of double fingers with very narrow grooves. A similar pattern was already obtained by Akamatsu *et al.* [7].

IV. CONCLUSIONS AND DISCUSSION

From our simulation of directional solidification, the tilting of a crystalline axis with anisotropic surface stiffness induces the tilting of the profile and the crystal grows in a direction different from the pulling direction. The tilt angle ϕ is shown to become large on increasing the pulling rate V, in agreement with the experimental observation [5–8]. There are, however, some aspects different from the experiment. In the ice experiment, the tilt angle ϕ depends weakly on ψ compared with our simulation for small ψ [8]. These discrepancies may be related to the kinetic effect, which is planned to be studied in a separate paper.

ACKNOWLEDGMENTS

The authors acknowledge discussions with Professor Y. Furukawa and K. Nagashima.

[1] J.S. Langer, in *Chance and Matter*, edited by J. Souletie, J. Vannimenus, and R. Stora (North-Holland, Amsterdam, 1987), p. 629.
[2] D.A. Kessler, J. Koplik, and H. Levine, Adv. Phys. **37**, 255 (1988).
[3] E. Brener and V.I. Mel'nikov, Adv. Phys. **40**, 53 (1991).
[4] Y. Pomeau and M. Ben Amar, in *Solids far from Equilibrium*, edited by C. Godrèche (Cambridge University Press, Cambridge, England, 1991), p. 365.
[5] R. Trivedi, V. Seetharaman, and M.A. Eshelman, Metall. Trans. **22A**, 585 (1991).
[6] A.G. Borisov, O.P. Fedorov, and V.V. Maslov, J. Cryst. Growth **112**, 463 (1991).
[7] S. Akamatsu, G. Faivre, and T. Ihle, Phys. Rev. E **51**, 4751 (1995).
[8] K. Nagashima and Y. Furukawa (unpublished).
[9] S.R. Coriell and R.F. Sekerka, J. Cryst. Growth **34**, 157 (1976).
[10] G.W. Young, S.H. Davis, and K. Brattkus, J. Cryst. Growth **83**, 560 (1987).
[11] Y. Saito, C. Misbah, and H. Müller-Krumbhaar, Phys. Rev. Lett. **63**, 2377 (1989).
[12] C.A. Brebbia, *The Boundary Element Method for Engineers* (Pentech, London, 1978).
[13] A. Classen, C. Misbah, H. Müller-Krumbhaar, and Y. Saito, Phys. Rev. A **43**, 6920 (1991).
[14] Y. Saito, G. Goldbeck-Wood, and H. Müller-Krumbhaar, Phys. Rev. Lett. **58**, 1541 (1987); Phys. Rev. A **38**, 2148 (1988).